Nuclear Inst. and Methods in Physics Research, A 902 (2018) 103–109

Contents lists available at ScienceDirect

Nuclear Inst. and Methods in Physics Research, A

journal homepage: www.elsevier.com/locate/nima

Development of a transmittance monitor for high-intensity photon beams

Y. Matsumura [1], T. Ishikawa *, Y. Honda, S. Kido, M. Miyabe, I. Nagasawa, K. Nanbu, H. Shimizu, K. Takahashi, Y. Tsuchikawa [2], H. Yamazaki [3]

Research Center for Electron Photon Science (ELPH), Tohoku University, Sendai 982-0826, Japan

ARTICLE INFO

Keywords:
Tagged photon
Tagging efficiency
Photon transmittance
Meson photoproduction
FPGA

ABSTRACT

A transmittance monitor has been developed for the second tagged-photon beamline at the Research Center for Electron Photon Science, Tohoku University, Japan. In this beamline, an internal radiator is employed to produce the bremsstrahlung photon beam out of circulating electrons in a synchrotron. The transmittance, which is defined as the probability of finding a photon coming to the target position when an electron is detected with a photon-tagging counter, should be determined to deduce cross sections for photo-induced reactions. The developed monitor consists of a telescope of thin plastic scintillators with a positron and electron converter, and a dedicated circuit implemented in a field-programmable gate array chip. The transmittance can be measured with this monitor for high-intensity photon beams corresponding to 20 MHz tagging signals. The measured transmittance is found to be constant with respect to the photon intensity for each photon-tagging channel.

1. Introduction

Photo-induced reactions with the incident energy ranging from several hundred MeV to a few GeV are important to study the structure of hadrons in detail. A hadron is a color-neutral object, and described in principle by quark and gluon dynamics as a solution of the fundamental theory of the strong interaction, quantum chromodynamics (QCD). At low energies, little is known for the solution owing to the large running QCD coupling constant. What are the effective degrees of freedom describing hadrons is a subject of interest associated with the color confinement problem. Meson photoproduction experiments have been conducted [1–5] to give information on the subject with an electromagnetic-calorimeter (EMC) system, FOREST [6], on the second photon beamline [7] at the Research Center for Electron Photon Science (ELPH), Tohoku University, Japan. Fig. 1 shows a schematic view of the second photon beamline at ELPH.

Bremsstrahlung photons are generated by inserting a thin carbon fiber (radiator) with a diameter of 11 μm into circulating electrons [7] in the electron synchrotron called Booster STorage (BST) ring (previously known as the STB ring) [8]. The energy of each photon is determined by measuring the momentum of its corresponding post-bremsstrahlung electron with a tagging detector system, STB-Tagger II [7], having 116 photon-tagging channels. Each tagging signal is produced from a telescope of two scintillating fibers with a cross section of 4×4 mm^2, covering a photon energy with a width of 0.5–2.8 MeV (σ). The tagging signal does not always correspond to a photon arriving at the target. Some of the tagged photons may be converted into a positron and electron (e^+e^-) pair owing to the material on the photon beamline. These undesirable e^+e^- pairs are swept out with a dipole magnet, $\mathcal{R}$TAGX [9], which is placed in front of FOREST. Furthermore, a photon is not generated when Møller scattering or Coulomb multiple scattering takes place at the radiator, but the scattered electron might hit a tagging detector. Therefore, the photon transmittance (so called the tagging efficiency), which is defined as the probability of finding a photon coming to the target position when an electron is detected with a tagging detector, should be determined to deduce cross sections for photo-induced reactions. The transmittance is experimentally measured since it is difficult to incorporate all the conditions of circulating electrons in the calculation.

So far, we have measured the transmittance, T_γ, using an EMC module on the photon beamline. The energy of a photon is measured with the module in response to the tagging signal. The singles rate of the module should be reduced so that it could work, namely the photon-beam intensity should be much lowered. Thus, we make the circulating current in the BST ring very low during the transmittance measurement. We describe a photon beam in this condition as a faint beam. To deduce

* Corresponding author.
E-mail address: ishikawa@lns.tohoku.ac.jp (T. Ishikawa).
[1] Present address: Research Center for Nuclear Physics (RCNP), Osaka University, Ibaraki 567-0047, Japan.
[2] Present address: Department of Physics, Nagoya University, Nagoya 464-8602, Japan.
[3] Present address: Radiation Science Center, High Energy Accelerator Research Organization (KEK), Tokai 319-1195, Japan.

https://doi.org/10.1016/j.nima.2018.06.025
Received 30 March 2018; Received in revised form 4 June 2018; Accepted 9 June 2018

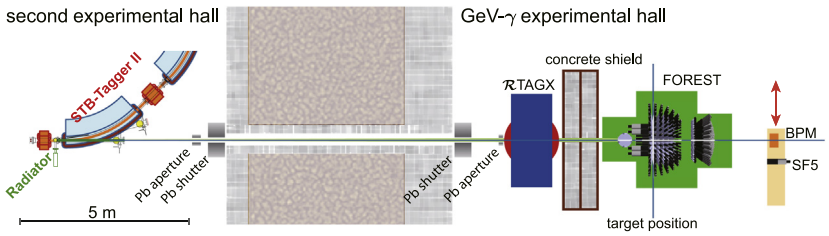

Fig. 1. Schematic view of the second photon beamline at ELPH. An electron synchrotron called Booster STorage (BST) ring [8] (previously known as the STB ring) and a photon-tagging detector, STB-Tagger II [7], are located in the second experimental hall. A charge sweeping magnet, $\mathcal{R}$TAGX [9], and a detector system, FOREST [6], are placed in the GeV-γ experimental hall. The photon-beam profile monitor with scintillating-fiber hodoscopes (BPM) [10] and an SF5 lead-glass Cherenkov counter for the photon-transmittance measurement can be inserted into the beamline by moving a stage horizontally. The diameters of the two lead apertures located in the second and GeV-γ experimental halls were 20 and 25 mm in the present work, respectively.

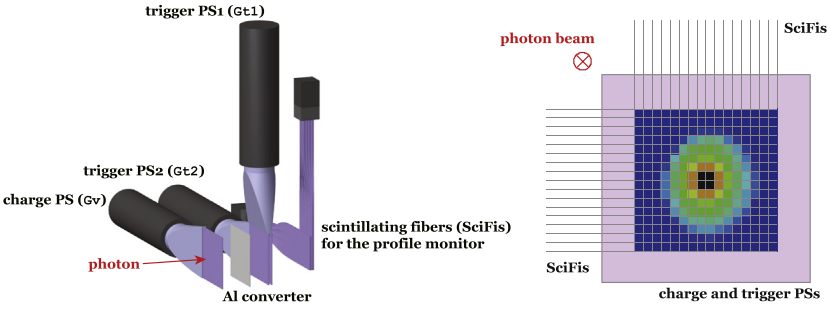

Fig. 2. Schematic view (left) of the detector system for the transmittance measurement together with its front view (right). It consists of three PSs with a thickness of 1 mm and an area of 70×70 mm^2. A 0.5 mm-thick aluminum plate is used as an e^+e^- converter. Additional two scintillating-fiber hodoscopes to give the intensity map of the photon beam at the target position are not used. A measured photon-beam profile taken from Fig. 11 in Ref. [10] is overlaid in the front view.

the differential and total cross sections for meson-photoproduction reactions measured with the high-intensity photon beams, the number of incident photons are given by the number of tagging signals and transmittance for each tagging channel. The values of the transmittance between the faint and high-intensity beams have been assumed to be the same so far. We have developed a transmittance monitor for high-intensity photon beams at normal operation (circulating current of $\sim$ 20 mA and photon-tagging rate of $\sim$ 20 MHz), and confirmed the transmittance is the same between the faint and high-intensity photon beams for each tagging channel.

2. Developed transmittance monitor

We used the same detector system for the photon-beam profile monitor with scintillating-fiber hodoscopes (BPM) [10]. BPM consisted of a plastic scintillator (PS) for charge veto (Gv), an aluminum-plate converter with a thickness of 0.5 mm, and two trigger PSs (Gt1 and Gt2). The thicknesses of the three PSs measured 1 mm each, and the number of trigger PSs was different from that in Ref. [10]. Each PS was covered by a Tyvek-1073D sheet (reflector) with a thickness of 0.19 mm, and a black sheet (light shielding) with a thickness of $\sim$ 0.2 mm. The coverage of each PS with an area of 70×70 mm^2 was sufficient since the width of the delivered photon beam was $\sim$ 8 mm (σ) [10]. Additional two layers of scintillating-fiber hodoscopes to give the intensity map of the photon beam at the target position were not used for the developed transmittance monitor. Fig. 2 shows the schematic view of the detector system for the transmittance measurement. The condition of finding a photon by this detector system (BPM trigger) was described as

$$\mathtt{Tr} = \overline{\mathtt{Gv}} \otimes \mathtt{Gt1} \otimes \mathtt{Gt2}, \tag{1}$$

where $\otimes$ stands for coincidence of signals. The Gv signal rejected the events in which charged particles were produced upstream, and the Gt1 and Gt2 signals required the events having an e^+e^- pair before passing through the two trigger PSs. The discriminator thresholds for producing logic signals of Gv, Gt1, and Gt2 were set to $0.5V_{\rm mip}$, $1.5V_{\rm mip}$, and $1.5V_{\rm mip}$, respectively. Here $V_{\rm mip}$ denotes the pulse height in response to the minimum ionizing particles. Only a fraction of the incident photon beam was converted in the aluminum plate into e^+e^- pairs. Since the BPM detector itself is sensitive only to charged particles (e^+e^- pairs) produced downstream of Gv, this fraction (sampling ratio), η_γ, affects the probability of finding a photon in the BPM detector corresponding to a tagging signal (BPM-response probability), R_γ. The actual photon transmittance, T_γ, can be determined from R_γ and η_γ:

$$T_\gamma = \frac{R_\gamma}{\eta_\gamma}. \tag{2}$$

Since T_γ is directly measured for a faint beam with an EMC module on the beamline, η_γ can be determined from the measured T_γ and R_γ values in the same condition. The determination of η_γ will be discussed in Section 3.

A circuit to give R_γ^i for each tagging channel i has been implemented into a developed NIM module called MPLM4. MPLM4 is a prototype of MPLM4X in Ref. [10] containing a field-programmable gate array (FPGA) chip, Xilinx Spartan-6 [11]. MPLM4 (MPLM4X) accepts and produces NIM standard signals through 36 (38) input and 18 output channels. The logical circuit has been designed using edge-aligned signals with an internal 200-MHz clock signal. The R_γ^i is determined by the numbers, Ns, of three signals for each tagging channel Tci:

$$R_\gamma^i = \frac{N(\mathtt{Tc}i \otimes \mathtt{Tr}) - N(\mathtt{Tc}i \otimes \mathtt{Tr}')}{N(\mathtt{Tc}i)}, \tag{3}$$

where Tr' denotes the 165-ns delayed signal for Tr, and the coincidence widths are the same between Tc$i\otimes$Tr and Tc$i\otimes$Tr'. The harmonic number of the BST ring with an RF frequency of 500.14 MHz is 83 [8]. The 165-ns delay approximately corresponds to the time of a revolution in the BST ring. Fig. 3 shows the diagram describing the operation of the transmittance monitor. The logic signals of Gv, Gt1, and Gt2 from the BPM detector, and those of 32 tagging channels out of 116 [7] are delivered to MPLM4.

The Tr signal is generated in the trigger generator component from Gv, Gt1, and Gt2 signals. The signal width is 8 clock cycles (40 ns)

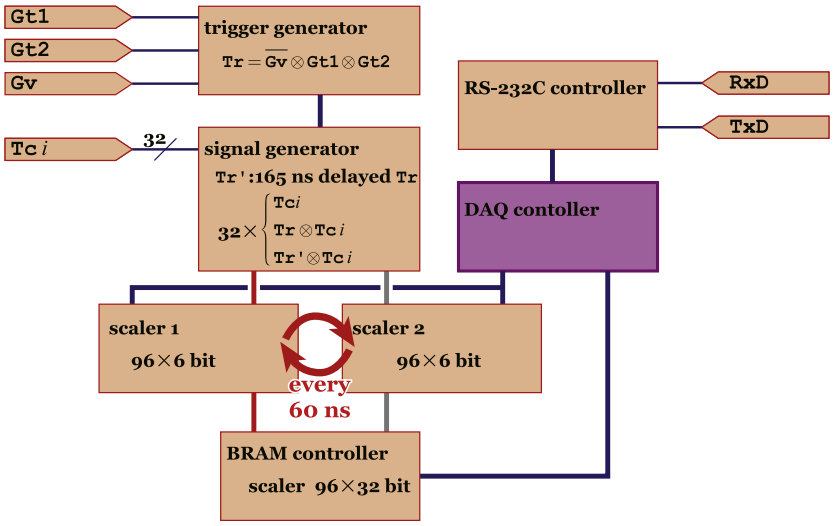

Fig. 3. Diagram describing the operation of the transmittance monitor. The trigger condition (BPM response) $\mathtt{Tr} = \overline{\mathtt{Gv}} \otimes \mathtt{Gt1} \otimes \mathtt{Gt2}$ is investigated in the trigger generator component. The $\mathtt{Tc}i \otimes \mathtt{Tr}$ and $\mathtt{Tc}i \otimes \mathtt{Tr}'$ signals are generated in the signal generator component for each tagging channel $\mathtt{Tc}i$, where $\mathtt{Tr}'$ denotes the 165-ns delayed signal for $\mathtt{Tr}$. The numbers of three signals $N(\mathtt{Tc}i)$, $N(\mathtt{Tc}i \otimes \mathtt{Tr})$, and $N(\mathtt{Tc}i \otimes \mathtt{Tr}')$ are counted in the two 96-channel 6-bit scalers. A scaler counts the numbers for all the 96 signals, and another scaler transfers the scaler data to the 96-channel 32-bit scaler implemented in BRAM using the BRAM controller component. The two scalers are exchanged with one another every 60 ns. The DAQ controller is interfaced with a personal computer through an RS-232C communication controller.

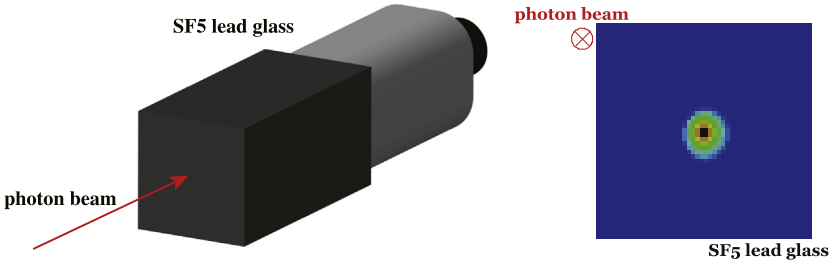

Fig. 4. Schematic view (left) of the SF5 detector for the transmittance measurement together with its front view (right). The thickness and area of the SF5 detector are 300 mm, corresponding to 11.8 in the radiation-length unit, and 150 × 150 mm^2, respectively. A measured photon-beam profile taken from Fig. 11 in Ref. [10] is overlaid in the front view.

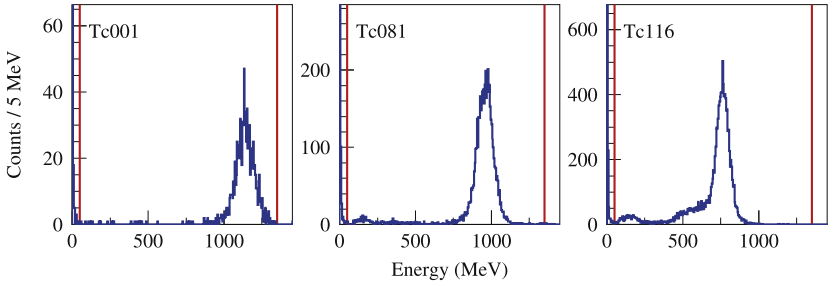

Fig. 5. Typical energy spectra of the tagged photons (6-kHz tagging rate). A single peak corresponding to the tagging energy can be observed, and low-energy components are included in some small fraction. The tagging channels $\mathtt{Tc001}$, $\mathtt{Tc081}$, and $\mathtt{Tc116}$ correspond to the energies of 1.26, 1.06, and 0.82 GeV, respectively.

for $\mathtt{Gv}$, and that is 4 clock cycles (20 ns) for $\mathtt{Gt1}$ and $\mathtt{Gt2}$. The leading edges of $\mathtt{Gt1}$ and $\mathtt{Gt2}$ signals are adjusted to be delayed by 10 ns with respect to $\mathtt{Gv}$. The numbers of three signals $N(\mathtt{Tc}i)$, $N(\mathtt{Tc}i \otimes \mathtt{Tr})$, and $N(\mathtt{Tc}i \otimes \mathtt{Tr}')$ are counted in the scaler components for each tagging channel $\mathtt{Tc}i$. Two 96-channel 6-bit scalers are prepared to remove the dead time for transferring buffered data by a double-buffer readout. A scaler component counts the number of hits in 96 generated signals, and another scaler transfers the scaler data to the 96-channel 32-bit scaler implemented in a block RAM (BRAM) using the BRAM controller component. The two scalers are exchanged with one another every 60 ns. The data acquisition (DAQ) controller is interfaced with a personal computer through an RS-232C communication controller. The DAQ system itself does not have a dead time for processing an event, however some counting loss takes place owing to the finite widths of signals and coincidences at high-intensity conditions.

3. Transmittance measurement

First of all, the sampling ratio, η_γ, was determined using faint beams with tagging rates of 1 and 6 kHz. We describe the rate for all the tagging signals simply as the tagging rate. The circulating energy of the BST ring was 1.32 GeV. The transmittance, T_γ, was measured by using an

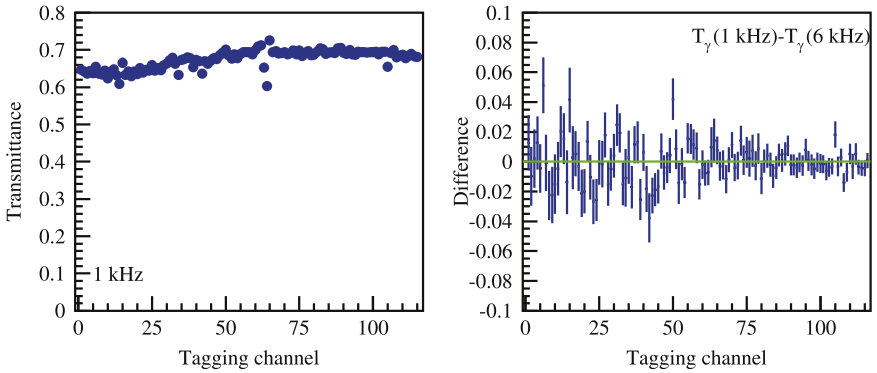

Fig. 6. Measured transmittance, T_γ, for the 1-kHz tagging rate (left) and difference of the measured transmittances between 1- and 6-kHz tagging rates (right).

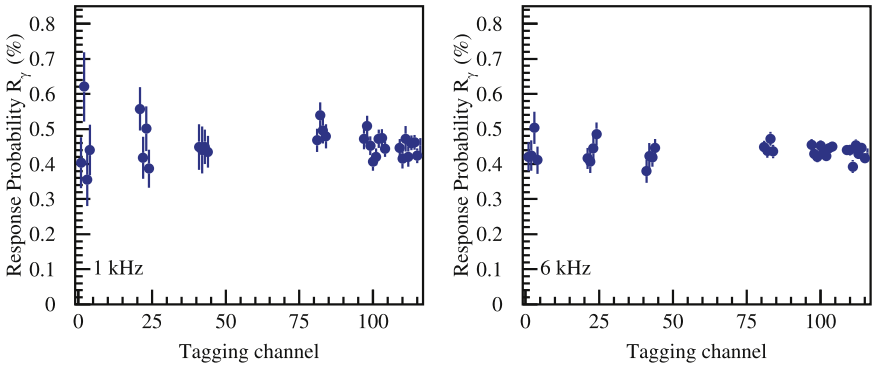

Fig. 7. Measured BPM-response probability as a function of the tagging channel for faint beams with tagging rates of 1 (left) and 6 kHz (right).

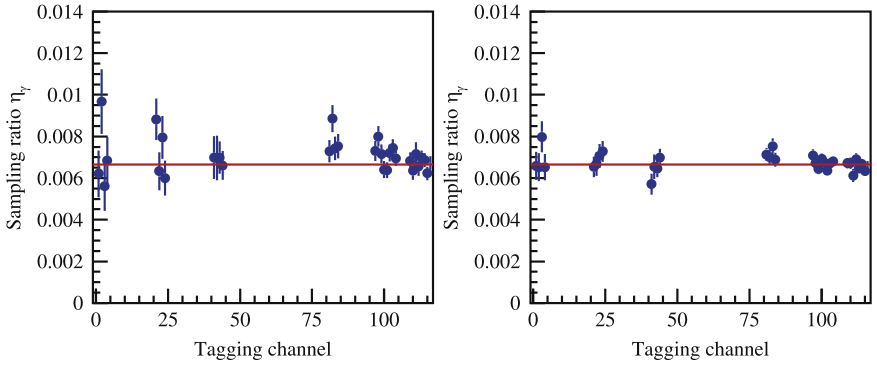

Fig. 8. Sampling ratio, η_γ, measured by using faint beams with tagging rates of 1- (left) and 6-kHz (right). The measured η_γs are compared with the expected value of 0.00665.

SF5 lead-glass Cherenkov detector [12] on the photon beamline, and the probability of the BPM response, R_γ, was measured in the same condition using the developed circuit in MPLM4. The ratio between these two values T_γ/R_γ corresponds to η_γ.

The transmittance measurement with the SF5 detector was carried out using the standard FOREST DAQ system described in Ref. [6]. The trigger for the DAQ was the OR signal of all the tagging channels. The SF5 detector gave the energy of the bremsstrahlung photons. Its thickness was 300 mm corresponding to 11.8 in the radiation-length unit, giving an efficiency of approximately 100%. Its cross section was 150 × 150 mm^2, covering all the area of the delivered photon beam. Fig. 4 shows the schematic view of the SF5 detector for the transmittance measurement. We adjusted the circulating current in the BST ring so that the counting rate of the SF5 detector would not exceed 50 kHz to make it work. Undesirable charged particles generated upstream of the target position for meson photoproduction experiments were swept out with a dipole magnet, $\mathcal{R}$TAGX [9]. We placed the SF5 detector on the photon beamline during the transmittance measurement (approximately 3-m downstream of the target position for meson photoproduction experiments).

The transmittance determined by the SF5 detector, $T_\gamma^{i\ (\mathrm{SF5})}$, for the ith tagging channel was given as

$$T_\gamma^{i\ (\mathrm{SF5})} = \frac{N_\gamma^i}{N_T^i}, \tag{4}$$

where N_T^i is the number of events detected with the ith tagging counter, which is equivalent to $N(\mathrm{T}ci)$ in the FPGA circuit. In Ref. [7], the number of events obtained without inserting the radiator was subtracted from N_T^i to avoid the contribution of the residual radioactivity around the yoke of the bending magnet where the tagging detector was placed. Faint beams with relatively higher intensity were employed in the present work so that the residual-radioactivity contribution should be

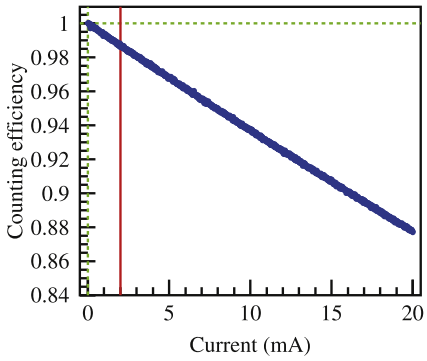

Fig. 9. Estimated counting efficiency of the BPM response owing to the finite signal widths as a function of the circulating current in the BST ring. The solid vertical line shows the 2-mA current which gives the counting rate for each element of the BPM detector.

negligibly small. Fig. 5 shows the measured energy spectra of the tagged photons. A single peak corresponding to the tagging energy can be observed, and low-energy components are included owing to the electrons from the Coulomb scattering or electromagnetic shower produced in the frame and supporting rods of the vacuum chamber [7] of the BST ring in front of STB-Tagger II.

The transmittance should be determined excluding this low-energy component for physics analysis. Since BPM consisting of thin PSs could not separate them, the transmittance here was determined including them. Fig. 6 shows the measured transmittance for the 1-kHz tagging rate, and difference of the measured transmittances between 1- and 6-kHz tagging rates. The measured transmittance is higher than that in Ref. [7]. This is because the circulating energy was increased from 1.2 to 1.32 GeV giving a smaller cone for bremsstrahlung photons, and because the diameter of the lead aperture in the second experimental hall in this measurement (20 mm) was larger than that in Ref. [7] (10 mm). The diameter of the lead aperture in the GeV-γ experimental hall was 25 mm. The difference of the measured transmittances between the 1- and 6-kHz tagging rates is found to have a constant value of -0.0010 ± 0.0009, and we have found no significant difference of measured photon transmittances between the two faint beams.

The BPM-response probability, R_γ^i, was measured using the developed circuit and determined by using Eq. (3). Fig. 7 shows the measured BPM-response probability as a function of the tagging channel for faint beams. We estimated the sampling ratio, η_γ, from the ratio of the measured values, $R_\gamma^i / T_\gamma^{i\ (\mathrm{BPM})}$ for each tagging channel. Since charged particles produced downstream of the target for meson photoproduction experiments were vetoed only for the BPM responses, each $T_\gamma^{i\ (\mathrm{BPM})}$ value is slightly lower than the actual $T_\gamma^i = T_\gamma^{i\ (\mathrm{SF5})}$. Each $T_\gamma^{i\ (\mathrm{BPM})}$ value was determined as

$$T_\gamma^{i\ (\mathrm{BPM})} = \alpha_{\mathrm{att}} T_\gamma^{i\ (\mathrm{SF5})}, \tag{5}$$

where α_{att} denotes the attenuation factor of 0.9962 corresponding to the probability of e^+e^- production of a photon passing through the material between the target and BPM detector, two 12.5-μm-thick Aramid windows for the target, a 100-μm-thick Mylar window of the vacuum chamber, and ~1.5-m-length air from the end of vacuum chamber to the detector. Fig. 8 shows the sampling ratio η_γ as a function of the tagging

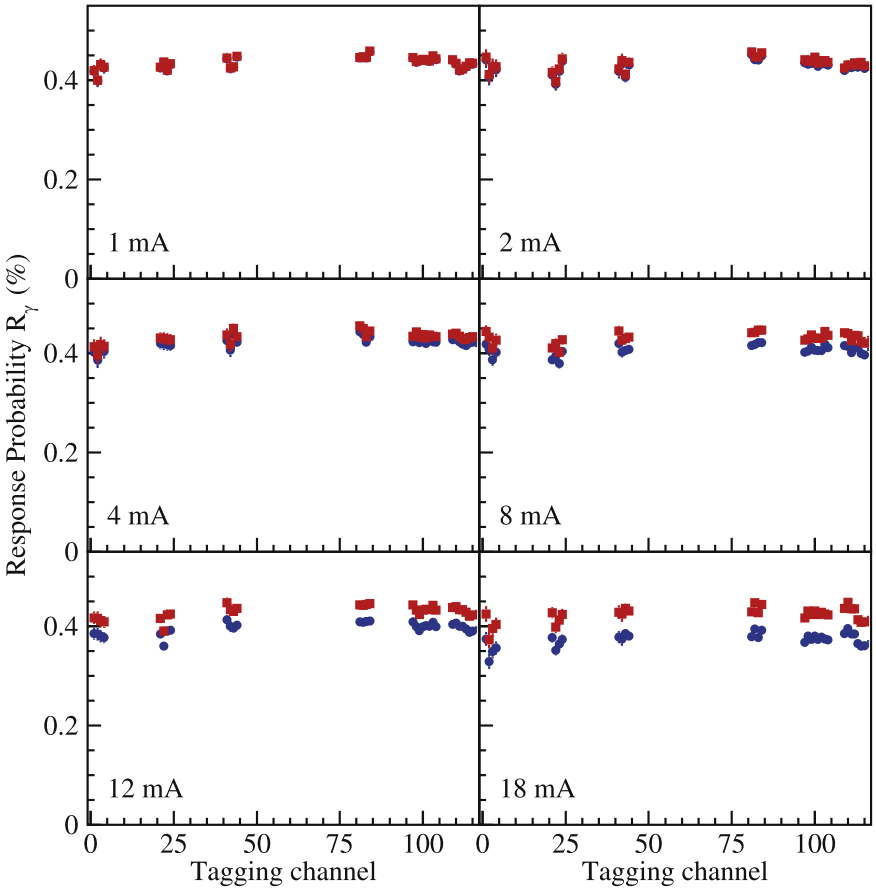

Fig. 10. BPM-response probability, R_γ, as a function of the tagging channel for high-intensity photon beams. The filled circles (blue) show the fraction of finding the BPM response to the number of photon-tagging signals, and the filled boxes (red) show the ratio after correction taking into account the counting-loss effect owing to the finite widths of signals. (For interpretation of the references to color in this figure legend, the reader is referred to the web version of this article.)

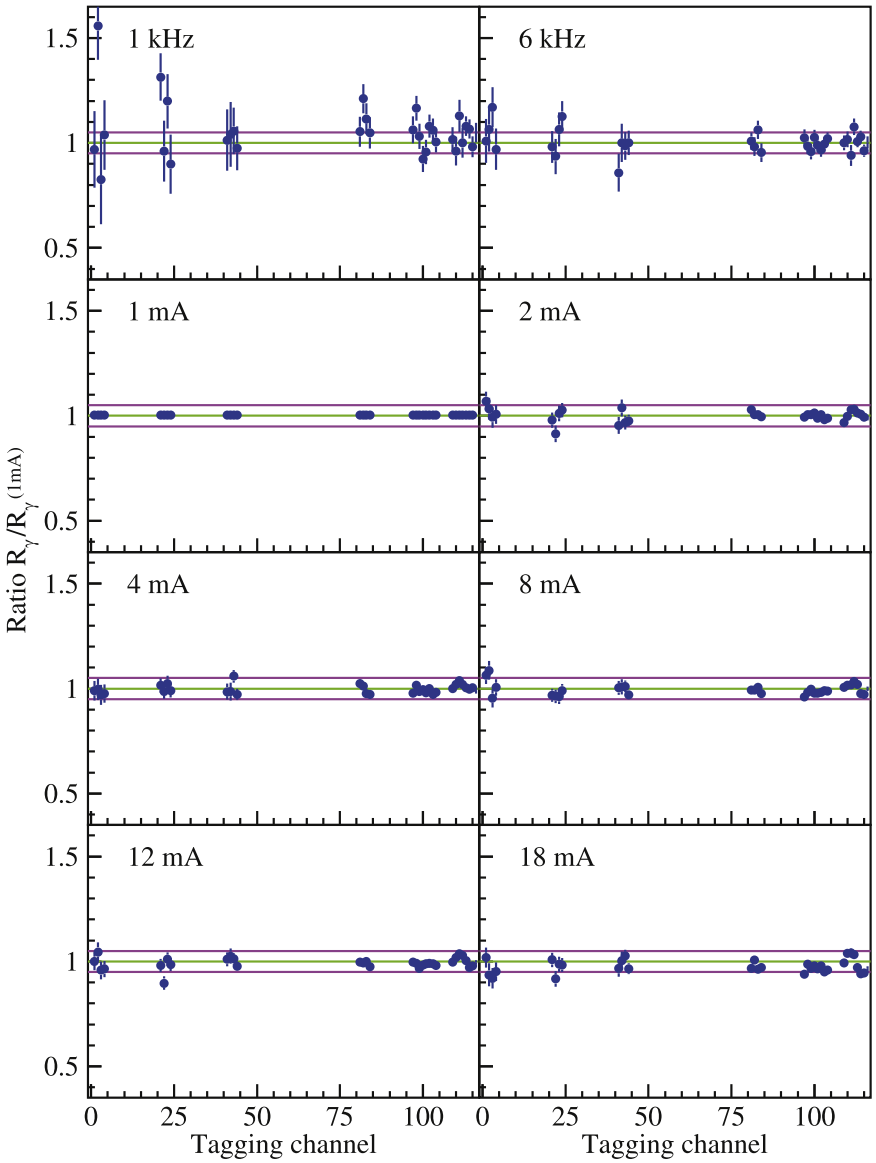

Fig. 11. The ratio of response probabilities of BPM. The measured response probability, R_γ, is divided by that for the circulating current of 1 mA. The three horizontal lines correspond to the ratio of 0.95, 1.00, and 1.05. The tagging rate of 1 kHz approximately corresponds to the circulating of 1 μA.

channel. The η_γ is found to be constant, and average values obtained are 0.00673 ± 0.00033 and 0.00662 ± 0.00020 for the 1- and 6-kHz tagging rates, respectively. These values are consistent with the expected value of 0.00658 ± 0.00015(thr) ± 0.00022(mat) for the sampling ratio, which is determined by a Monte-Carlo simulation based on Geant4 [13]. The errors 0.00015(thr) and 0.00022(mat) are given by the uncertainty of the effective discriminator threshold values (±20%) and that of the material thickness covering each PS (±0.05 mm), respectively. Since the measured value of η_γ includes the uncertainty of the material thickness, we have adopted the average value 0.00665 ± 0.00017 with a systematic uncertainty of 0.00015 for the measured sampling ratio.

In the second step, we investigated the measured transmittances at the various tagging rates. Since the constant value of η_γ has been determined by using faint beams, the transmittance for each tagging channel can be obtained as

$$T_\gamma^i = \frac{T_\gamma^{i\ (\mathrm{BPM})}}{\alpha_{\mathrm{att}}} = \frac{R_\gamma^i}{\alpha_{\mathrm{att}}\eta_\gamma}. \tag{6}$$

Since the counting loss takes place in the BPM response at high intensity owing to the finite width of input signals, the measured R_γ^i should be corrected. At first, the counting-loss effect was investigated using a Monte-Carlo simulation. In the simulation, all the signals were generated in response to a photon arrival (uniformly distributed in time) to the BPM detector. The `Gv`, `Gt1`, and `Gt2` signal rates were proportional to the circulating current, and those at 2 mA were the same as measured values 0.144, 0.240, and 0.323 kHz, respectively. The signal generation was checked every 5 ns according to the probability corresponding to the singles rate, the generated signal widths were set to 40 ns for `Gv`, and 20 ns for `Gt1` and `Gt2`. The `Gt1` and `Gt2` responses were delayed by 10 ± 5 ns with respect to `Gv`, where −5-, 0-, +5-ns time jitters were given randomly with equal probability. Two signals with an interval of less than 15 ns were unified to a single signal. Fig. 9 shows the estimated counting efficiency of the BPM response as a function of the circulating current in the BST ring. The counting efficiency drops linearly as a function of the circulating current in the BST ring.

We measured the BPM-response probabilities for the six circulating currents of 1, 2, 4, 8, 12, and 18 mA. Since the circulating currents given by a DC current transformer (DCCT) did not have enough accuracy, the ratio of the measured tagging rates were employed for that of photon intensities. The ratio of photon intensities for 1, 4, 8, 12, and 18 mA to the intensity at 2 mA were found to be 0.286 ± 0.010, 1.970 ± 0.022, 4.445 ± 0.045, 6.152 ± 0.062, and 9.535 ± 0.096, respectively. The actual

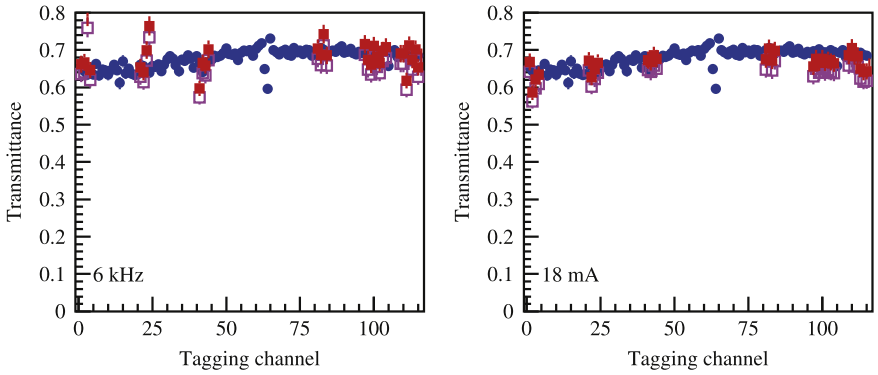

Fig. 12. Transmittance, T_γ, measured with BPM at 6-kHz tagging rate (left) and at 18-mA circulating current (right). The filled circles (blue) show T_γ measured with the SF5 detector at 1-kHz tagging rate. The open (magenta) and filled (red) boxes show T_γ determined by using η_γ = 0.00665 and 0.00640, respectively, from the measured R_γ with BPM. The measured η_γ by using the faint beams is $0.00665 \pm 0.00017(\text{sta.}) \pm 0.00015(\text{sys.})$. (For interpretation of the references to color in this figure legend, the reader is referred to the web version of this article.)

currents of 1, 4, 8, 12, and 18 mA were approximately 0.6, 3.9, 8.9, 12.3, and 19.1 mA, respectively, if the circulating current of 2 mA was correctly measured. The counting efficiency of the BPM response for each circulating current was obtained using these values. Fig. 10 shows the BPM-response probability, R_γ, as a function of the tagging channel for high-intensity photon beams. Similar R_γ values are obtained for different circulating currents after correcting the counting-loss effect.

Since η_γ must be constant, the transmittance as a function of the circulating current can be observed in the measured BPM-response probability. Fig. 11 shows the ratio of BPM-response probability to that obtained in the 1-mA circulating current. The obtained ratios of the BPM-response probabilities have a constant value in a range from 0.95 to 1.05 including the results from the faint beams. Thus, the measured transmittance for each tagging channel is constant independently of the circulating current (photon intensity). The actual transmittance, T_γ^i, can be obtained dividing the BPM-response probability, R_γ^i, by the sampling ratio $\eta_\gamma = 0.00665 \pm 0.00017 \pm 0.00015$ and attenuation factor α_{att}. Fig. 12 shows the finally deduced T_γ measured with BPM at 6-kHz tagging rate and at 18-mA circulating current. The T_γ measured with BPM is consistent with that with the SF5 detector within the errors corresponding to the uncertainty of η_γ.

4. Summary

A photon-transmittance monitor has been developed for the second tagged-photon beamline at ELPH. The developed monitor consists of a telescope of thin plastic scintillators with an e^+e^- converter, and a dedicated circuit implemented in an FPGA-based logic module. The transmittance, T_γ, can be obtained from the response probability of the detector, R_γ, and sampling ratio (the probability of e^+e^- production with the converter), η_γ. The η_γ is determined using faint beams by comparing the R_γ and directly measured T_γ with an EMC module. The η_γ is found to be $0.00665 \pm 0.00017(\text{sta.}) \pm 0.00015(\text{sys.})$. The R_γ can be successfully measured with this monitor for high-intensity photon beams corresponding to 20 MHz tagging signals. The measured R_γ is found to be constant with respect to the photon intensity for each photon-tagging channel within the statistical error (approximately ±5%). This suggests that T_γ is constant independently of the circulating current. The accuracy of the transmittance measured at high intensity is expected to be ±5% owing to the uncertainty of η_γ.

Acknowledgments

The authors wish to thank the ELPH accelerator staff for providing the primary electron beam in stable condition. This work was supported in part by Grants-in-Aid for Scientific Research (A) No. 24244022, for Scientific Research (C) No. 26400287, and for Scientific Research (A) No. 16H02188.

References

[1] T. Ishikawa, et al., Phys. Lett. B 772 (2017) 398.
[2] T. Ishikawa, et al., Proceedings of the XV international conference on hadron spectroscopy-hadron, in: PoS(Hadron 2013), p. 095.;
T. Ishikawa, et al., Proceedings of the 10th international workshop on the physics of excited nucleons (NSTAR2015), JPS Conf. Proc. 10 (2016) 031001.
[3] Y. Tsuchikawa, et al., Proceedings of the 12th international conference on hypernuclear and strange particle physics (HYP2015), JPS Conf. Proc. 17 (2017) 062007.
[4] T. Ishikawa, et al., Proceedings of the 26th international nuclear physics conference, in: PoS(INPC2016), p. 267.
[5] S.X. Nakamura, H. Kamano, T. Ishikawa, Phys. Rev. C 96 (2017) 042201 (R);
T. Ishikawa, et al., Acta Phys. Polon. B 48 (2017) 1801.
[6] T. Ishikawa, et al., Nucl. Instrum. Methods A 832 (2016) 108.
[7] T. Ishikawa, et al., Nucl. Instrum. Methods A 622 (2010) 1.
[8] F. Hinode, et al., Proceedings of 11th international conference on Synchrotron Radiation Instrumentation, SRI2012, J. Phys.: Conf. Ser. 425 (2013) 072011;
F. Hinode, et al., Proceedings of the 7th International Particle Accelerator Conference, IPAC2016, p. 701.
[9] K. Maruyama, et al., Nucl. Instrum. Methods A 376 (1996) 335;
T. Ishikawa, et al., Nucl. Instrum. Methods A 694 (2012) 348.
[10] T. Ishikawa, et al., Nucl. Instrum. Methods A 811 (2016) 124.
[11] Spartan-6 Website, http://www.xilinx.com/products/silicon-devices/fpga/spartan-6.html.
[12] A. Ando, et al., KEK Report, 1979, KEK-79-21.
[13] S. Agostinelli, et al., Nucl. Instrum. Methods A 506 (2003) 250;
J. Allison, et al., IEEE Trans. Nucl. Sci. 53 (2006) 270 Geant4 Website, http://geant4.cern.ch/.